Characterising Dynamic Performance of Automotive Sheet Metals for Improved Crash Design

Authors:

P.K.C. Wood, C. A. Schley, S. Kenny, I. McGregor[1], R. Bardenheier[2], T. Dutton[3], N. Heath[4]

University of Warwick, Premium Automotive Research and Development
[1]Corus Automotive
[2]Instron
[3]Dutton Simulation
[4]Jaguar and Land Rover

Correspondence:

International Automotive Research Centre
University of Warwick
Coventry
CV4 7AL

Telephone 02476 575379
Principal and Corresponding Author Email P.K.C.Wood@warwick.ac.uk

Keywords:
High velocity tensile testing, Analysis of errors, Crash material properties, Experimental simulation, Crash simulation, Model validation, Material characterisation

ABSTRACT

In conventional high velocity servo hydraulic testing systems, the strain rate effect we seek to measure in a material by testing specimens in tension is error prone, because it often drowned by inertia and noises arising from the machine testing and measurement system. This problem is acute in the industry. A new high velocity servo hydraulic test machine equipped with new gripping technology and an improved measurement system, which has a potential to reduce system error on the measured properties, was procured for this research. A preliminary step has been to establish the capability of this new test machine with the aim of minimizing system error. This paper describes this task in which the essential features of the test machine, specimen and system of measurement are modelled using finite element analysis and validated with experimental data. The purpose of the model is to gain an improved understanding of the physics involved in high speed tensile testing at 15 m/s, especially to identify the main sources of large error, and effective countermeasures as a pre-requisite to designing such tests.

INTRODUCTION

An improved understanding of the behaviour of automotive materials at high velocity is driven by the challenges of diverse crash legislation and competition amongst car makers. The strength of a sheet steel product is dependent on the speed at which it is deformed[1-5]. In the industry this is called strain rate effect and the higher the strain rate the higher the strength.

New advanced high strength steels are seen to be increasingly attractive in those parts of the body-in-white with demanding performance requirements leading to improved vehicle crashworthiness[6,7] and a potential for weight reduction. Design for performance must be matched with reliable material data as a basic input to simulation tools. This requirement is driven by the increasing sophistication of vehicle crash models in their numerical description. Uncertainty in the reliability of high speed tensile test data increases with strain rate and the cost of generating such data is also variable, generally the cost is high. In crash design the strain rate dependent properties of steel products must be determined accurately in the performance range of interest to end users. In response to this, this research is concerned with refinement and standardization of current testing, characterization and validation processes, leading to the economic generation of reliable strain rate dependent material data for use in crash simulation based design.

The first challenge must be how to generate reliable high speed tensile test data in the range of interest to the end user. The starting point for this task is to investigate existing vehicle crash models to identify important modes of crash behaviour in the vehicle body-in-white structure. From which representative component tests and loadings may be designed in isolation of the body-in-white to replicate these modes of behaviour. These components and loadings define the strain rate range of interest and typical strains attained during deformation under crash loads, but in addition, they will enable the high speed tensile data to be validated to discern the strain rate effect. Strain rates reached in component based simulation studies carried out in this project suggest the range of interest could be as high as 600 s^{-1} for local deformations, and around 50 s^{-1} for global deformation of the structure. The strain range of interest in the tensile curve is from yield point to maximum stress.

EXPERIMENTAL INVESTIGATIONS

Sources of Error

The figure 1 shows ten engineering stress strain curves derived from tension tests at low speed for a sheet steel product taken from the same coil, and tested in a common direction[8]. The data appears smooth and continuous exhibiting low variability. The source of this low variability is expected to be in the test system and system of measurement.

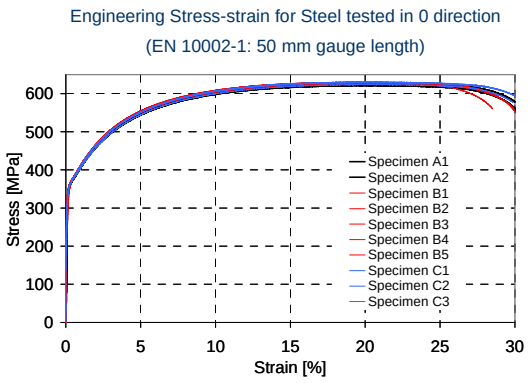

For the material tested, yield point is measured at 0.2% proof offset and maximum stress occurs at about 20% under quasi-static conditions[9].

High accuracy and precision in deriving point properties such as yield point over the range of interest is expected from such smooth data. Such low variability could not be achieved when testing at high velocity in conventional high speed servo-hydraulic test machine systems due to a wider variety of error sources, promoting high variability and therefore increased error unless a large number of tests are conducted and this of itself leads to difficulty with interpretation, and incurs high cost.

Sources of large error may arise from machine system effects, such as inertia in the grips or a heavy specimen, which may promote low variability only because system inertia masks all other sources of error. The measured data derived however would be unreliable. Another source of error may arise from the machine measurement system which is remote from the specimen. There is potential error in the interpretation of the raw test data, for example oscillations in the response, and the various transformation stages required to create a family of monotonically increasing flow curves is presently not well defined.

Experimental Equipment

A new state of art servo-hydraulic high speed test facility[10] has been procured to support this research project at the IARC. The main features of the test machine may be summarised:

- Actuator velocity: 10mm/s up to 20 m/s under open loop control (closed loop control up to 1 m/s) in tensile and compression
- Fast Jaw (gripping of specimen)
- Velocity profile correction
- Four column load frame
- Improved system of measurement at high frequency (sensors in m/c and on specimen, DAQ)

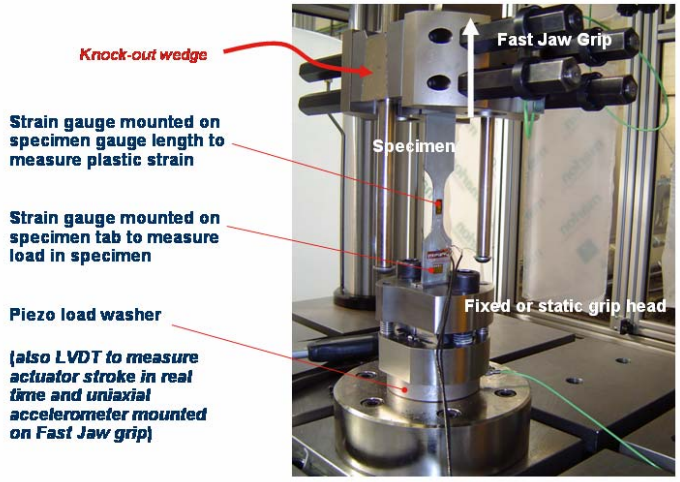

Figure 2: Tensile Specimen Assembled in High Velocity Servo-hydraulic Test Machine

The principle of operation requires the fast jaw grip to be accelerated in the direction of the white arrow in figure 2 to reach target velocity. The knock out wedge is kicked out by a spacer rod pre-set by the test requirements, the grips are released to grab the specimen in typically 5 μs (5×10^{-6} sec).

Sensors in the machine system include Piezo load washer in the static grip head to measure force transmitted to test machine, Linear variable differential transducer to measure actuator stroke position, and accelerometer mounted on the Fast Jaw. The signals from each of these sensors are recorded on a time base. Importantly strain gauges are placed on the specimen: one strain gauge placed at the centre of the gauge length will measure high elongation to derive true strain, whilst strain gauges on the wider section of the fixed tab end will enable a force measurement in this 'elastically' stretched zone to derive true stress. These specimen measurements may be compared with machine system placed sensors.

Specimen Design

Specimen design for high speed tensile testing is a function of two dependencies - machine capability and desired strain rate.

Figure 3: IARC Specimen Design for High Velocity Tensile Test at 15 m/s

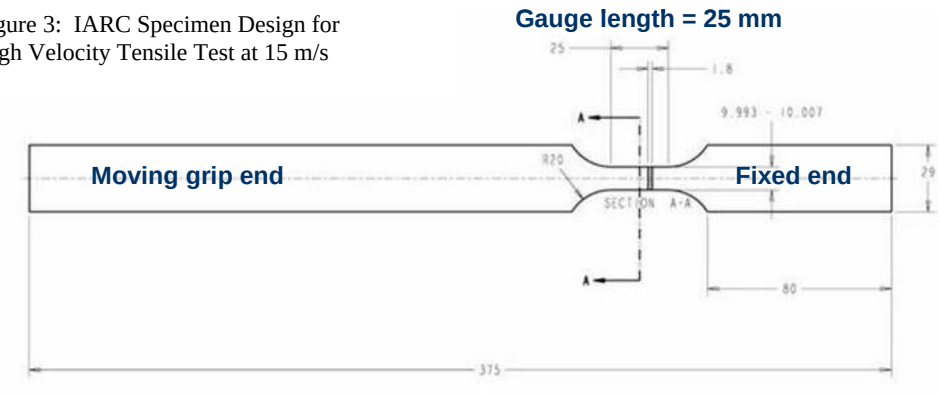

The conventional engineering strain rate is expressed by the formula grip velocity divided by initial gauge length[11]. The strain rate determined from this formula may be reasonable to a first approximation. The higher speed tensile specimen design shown has a gauge length of 25 mm, which may deliver a typical strain rate of 600 s^{-1} with an actuator velocity of 15 m/s. The short gauge length is expected to increase total elongation to failure.

The IARC specimen design shown is largely based on a review of international specimen designs but also match the capabilities of the new IARC facility. Especially avoiding very small gauge lengths that are a feature of a number of many other well known test laboratories. The low speed test data shown earlier conforms to the current Euronorm[9], which clearly describes the design of specimen and more generally the requirements for the tensile testing of metallic materials. A Euronorm for high velocity testing is not in place, although the IISI[12,13] has just published a first edition supplier based standard in September this year, listing recommendations for dynamic tensile testing of sheet steels.

Typical High Speed Tensile Test Data

The experimental data in the figure 4 plots the measured force output against actuator position with target grip speed in the test set to 15 m/s. The dashed blue line is the velocity variation of the actuator under open loop control without velocity profile correction. The actuator speed is observed to vary between 14.5 and up to 16 m/s. The average speed is computed at 15.1 m/s and the conventional engineering strain rate is determined at 605 s^{-1}. The output from the machine mounted force sensor (piezo load washer) is given by the red curve. A ringing frequency of around 6kHz is observed.

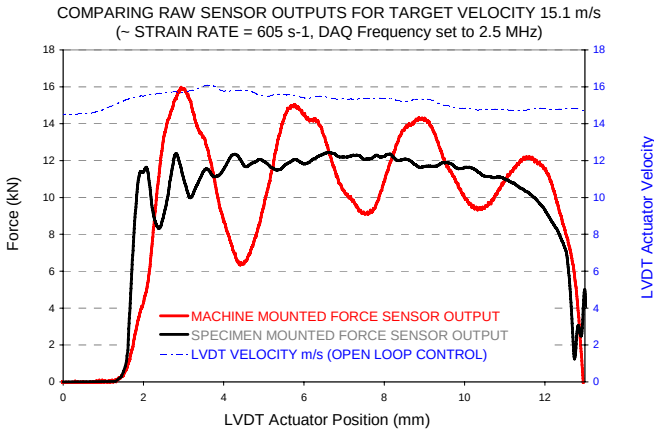

Figure 4: High Speed Test Data

The output from the strain gauge force sensor mounted on the specimen is given by the black curve. A higher oscillating frequency of around 23kHz is observed. The output from the specimen mounted force sensor shows a good fit through lower the frequency data measured by the machine mounted force sensor.

The strain gauge on the gauge length is designed to measure high elongation, typically up to 20% under quasi-static conditions, but currently attains a strain of around 3% before adhesive failure under dynamic load. Although the strain gauge adhesive achieves just 3%, this is still sufficient to pin point yield point with improved precision[14]. Investigations however continue[15] to improve this measurement. Regardless, we may still compute specimen gauge length extension without introducing a large error

using LVDT actuator position by using CAE. CAE will determine the compensation for the stretch of the specimen tabs ends held between fixed and moving grips and the transition zone to the gauge length.

Comparing Test Data at Low and High Strain Rate

In the figure 5, the lower blue curve measures low speed or quasi-static properties. The upper red curve measures the performance of the same material at a test speed of 15.1 m/s delivering a strain rate of 605 s^{-1}. Clearly a significant strain rate effect is observed comparing filtered upper curve with lower curve.

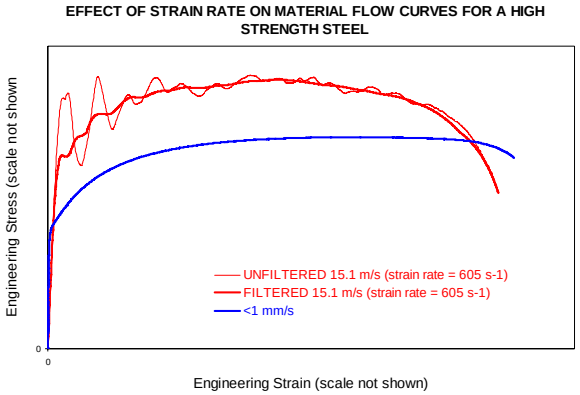

Figure 5: Measured Strain Rate Effect

NUMERICAL INVESTIGATIONS

Modelling Test

The purpose of simulating a high speed tensile test at 15 m/s is to gain an improved understanding of the physics involved, especially to identify the main sources of large error, and effective countermeasures as a pre-requisite to designing such tests. The sources of large error to be investigated;

- Specimen inertia
- System of measurement (e.g. sensors and positions)
- Interpretation of the information derived from the experiment (e.g. oscillation in the raw data curves)

A model of the specimen and important machine details to include all sensors in the measurement system and boundary conditions is shown in figure 6 below, using a commercially available software tool available to industry ~ Oasys LS Dyna[16].

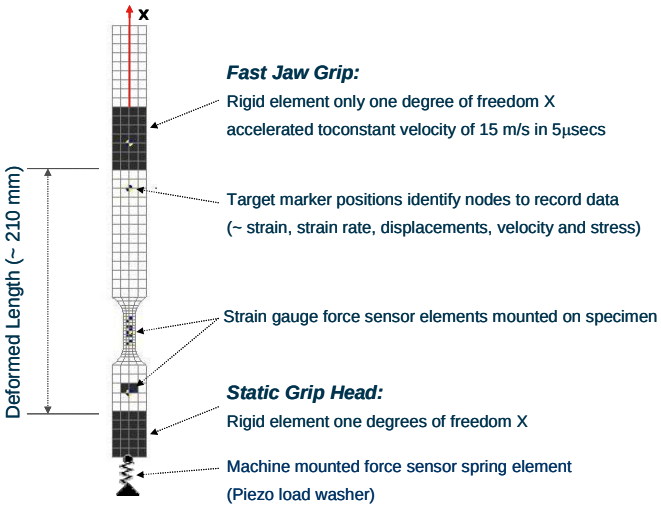

Figure 6: Model of Specimen, Sensors and Boundary Conditions

The fast jaw grip is shown in the clamp position and represented by a rigid element accelerated to target velocity of 15 m/s in 5μsec. At the lower end, the static grip head is represented by a rigid element and connected to a spring with the same stiffness as the machine mounted force sensor[17]. The total mass of the static grip head is estimated and lumped at the top of the spring, and this lumped mass is used to calibrate the frequency output from the machine mounted force sensor. Initially no damping is included in the model, but damping is used to calibrate the amplitude of the frequency output from the machine mounted force sensor. Two strain gauge force sensor elements mounted on specimen are represented by thin elastic shell elements.

Effect of Specimen Inertia

Although the specimen mass is low ~100g, a high acceleration which occurs in such tests may give rise to a large inertia force, which may result in an increase in the measured strength properties derived form the specimen under test even if the material is strain rate insensitive. This effect should be compensated through calibration, in which tests on the machine are conducted over a range of speeds, while a representative specimen clamped in the fast jaw grip remains unconnected to the static grip head, and the inertia force recorded to a calibration file. This practice must be carried out routinely.

In the model of the experiment, quasi-static material data is sufficient to test the effect of specimen inertia. The figure 7 plots two unfiltered curves. The hashed black curve is the stress - strain output from the model, measured from the centre node in the specimen as shown by the arrow to the target marker. The other solid red curve is the original quasi-static input data to the model. The result shows that model output equals model input and specimen inertia has no discernible effect.

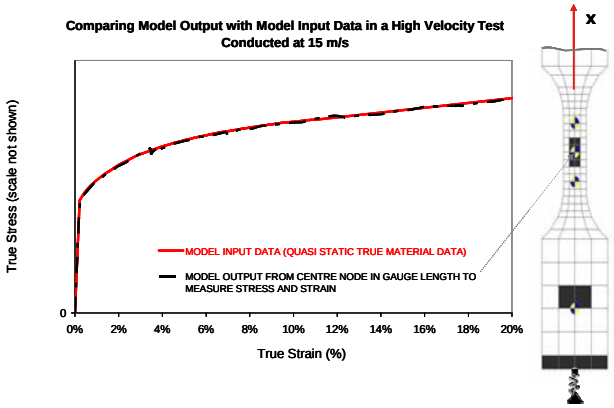

System of Measurement - Position of Strain Gauge Sensors on Specimen

Strain gauge sensors on specimen must be placed in fields of uniform strain. In figure 8, the lower specimen mounted strain gauge enables a force measurement to be derived in this elastically stretched zone, whilst the strain gauge mounted in the gauge length zone will enable a strain measurement during plastic deformation.

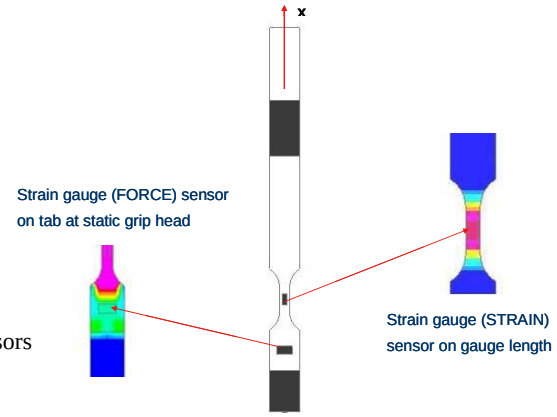

Figure 8: Position of Strain Gauge Sensors on Specimen

Velocity Profile across Specimen

The figure 9 shows a velocity profile exists across the specimen from the moving grip to the static grip head measured at the node positions indicated. Oscillations are observed. The velocity varies across the specimen from a maximum of 15 m/s at the moving grip to effectively zero at the static grip head. Therefore the specimen mounted force sensor measures a strain under low speed or effectively a quasi-static static condition. This is an important observation. The velocity profile across the gauge length varies from 13 m/s to just under 2 m/s.

Figure 9: Velocity Profile across

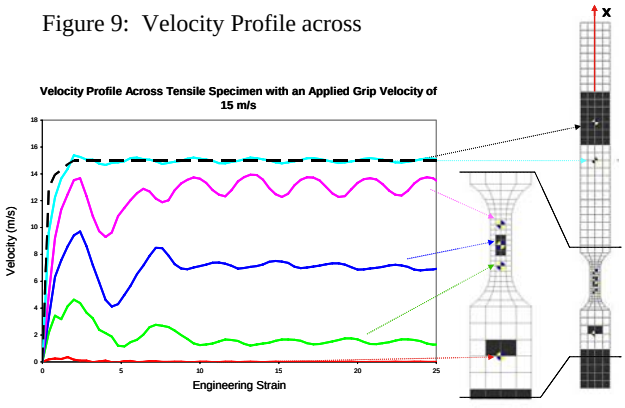

System of Measurement – Strain Rate Measured from Strain Gauge Sensors in Model

The figure 10 shows strain rate measured at the two specimen mounted sensor positions indicated. The output is oscillatory. The measured stain rate at the sensor on the gauge length varies between 340 and 550 s^{-1}, the average value computed is 414 s^{-1} in the strain range of interest. This is considerably lower than the design value computed at 600 s^{-1} for a test conducted at 15 m/s, using the simple formula - grip velocity divided by initial gauge length[11]. Although not shown, the strain rate variation measured across the gauge length at the three target positions shown, is much lower than the corresponding velocity variation observed across the gauge length. The strain rate measured from the strain gauge sensor at the lower grip is near zero.

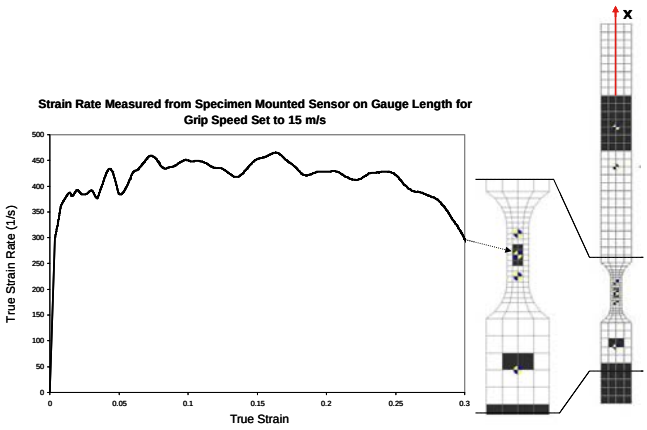

Figure 10: Strain Rate Measured from Specimen Mounted Sensor on Gauge Length

The important thing is that the strain rate dependent material data derived from such tests must be correctly related to the developed strain rate so that a family of strain curves for use in design may be validated.

Stress Wave Propagation

In testing at high velocity, a stress wave propagates in the specimen at the speed of sound in the material when load is applied[18,19]. For a thin steel specimen undergoing elastic uniaxial deformation, a stress waves travels at approximately 5200 m/s. Under plastic deformation this figure reduces significantly. The stress wave moves along the specimen and is reflected at free edges and boundary conditions, for example the transition zone at the gauge length and at the fixed grip as shown in the model.

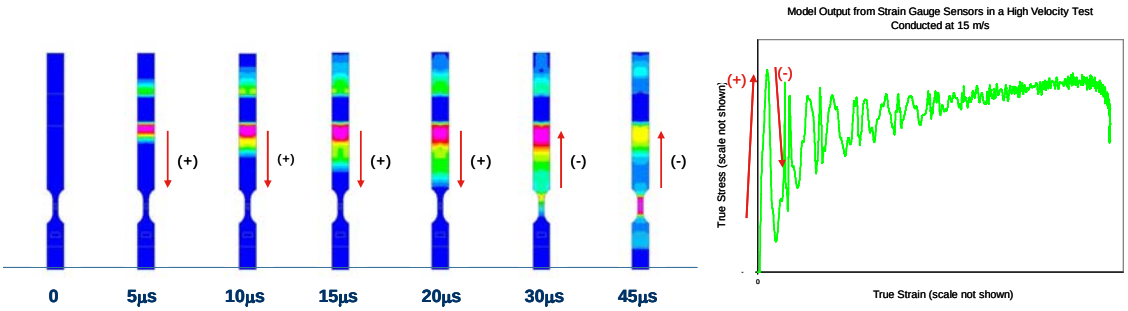

Figure 11: Movement of Stress Wave in Tensile Specimen on Load Take-up

The high frequency oscillation of 23 kHz observed in the specimen mounted force sensor in the fixed tab end of the specimen as shown in the graph appears to correspond to the motion of stress waves travelling back and forth through specimen. The wave length of the stress wave is roughly 210 mm and this corresponds to the initial length of the specimen between the fixed and moving grip. It is noted that in the time it takes a stress wave to reach the strain gauge sensor on the gauge length the moving tab end has stretched elastically by almost 0.5 mm for the applied grip speed of 15 m/s.

Calibrating Model Frequency Response from Machine Mounted Force Sensor

The final step in this investigation is to consider how to interpret the raw output from the various sensors yielding the test data, specifically, filtering the oscillatory response from the force sensors to create a

smooth monotonic curve. The interpretation of raw data of itself can lead to a very significant error even after introducing appropriate countermeasures to reduce error in the raw test data. To assist in the task of developing a suitable filtering technique and determine likely error, it is better to use simulated data. For this it is necessary to calibrate the frequency response of the model.

The figure 12 plots the force sensor output from test machine against actuator position for a nominal test speed of 15 m/s. The graph compares model and experimental data. The red curve is the force sensor output from the experiment and failure of specimen is observed, and the ringing frequency of 6 kHz decays with distance. The hashed green curve is the model output, which has been calibrated to deliver the same frequency output of 6 kHz as the experimental data by adding an effective mass of 22 kg to the top of the machine mounted spring element. The amplitude of the frequency response of the green hashed curve is attenuated through viscous damping being applied in the model to give the blue curve, which also shows the same rate of decay.

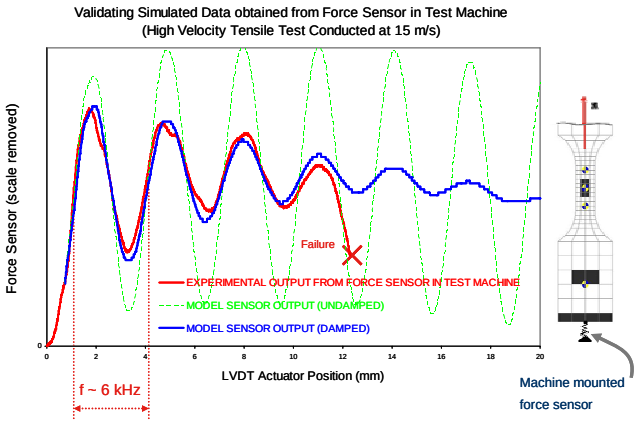

Figure 12: Frequency Response from Machine Mounted Force Sensor

The aim is to validate the model frequency response, not the actual force levels from the model and test. The force level determined from the model is lower than the experiment because quasi-static material data is used in the model, whereas test data at 15 m/s actually delivered a markedly higher force output due to the strain rate effect. The force level between model and test agree only because the model data was factored to match the experimental force output.

The figure 13 shows the force sensor output from the specimen mounted strain gauge and actuator position for a nominal test speed of 15 m/s. The horizontal scale is amplified because the frequency response of this sensor is much higher.

The red curve plots the force sensor output from the experiment and an oscillating frequency of 23 kHz is observed, which decays with distance. The dark hashed curve is the output from the machine mounted force sensor which has a much lower frequency, and provided for reference only. The hashed green curve is the model output, which has not been calibrated. The frequency of the model output is approximately 26 kHz, which is slightly higher than the experimental data, and the oscillations appear to correspond to movement of stress waves being reflected back and forth at the specimen boundary conditions.

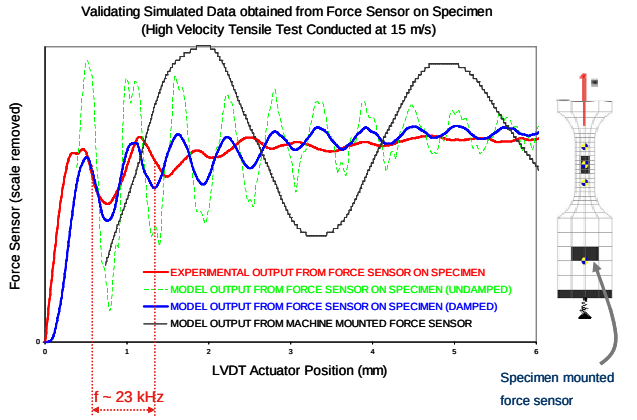

Figure 13: Frequency Response from Specimen Mounted Force Sensor

The amplitude of the green hashed curve is attenuated through damping, which is applied as a post-processing operation as shown by the blue curve.

Interpreting Data Output from Calibrated Model

The simulated data output from the specimen and machine mounted force sensors, is shown in the figure 14. This is derived true stress and true strain over the performance range of interest.

The green curve is the model output from the machine mounted force sensor and true strain derived from the strain gauge at the centre of the gauge length. The blue curve is the model output from the specimen mounted force sensor and true strain derived from the same strain gauge at the centre of the gauge length. The red curve is the material input data using a quasi-static material curve to provide a reference to compare model output data. The important thing to note is the fit of the model output data to the model input data. In the high velocity tensile test conducted on the machine the strain rate effect will shift the red curve up on the vertical axis, and it is this information that we seek to derive from the oscillatory curves obtained from a real high speed test, and create a smooth monotonically increasing flow curve.

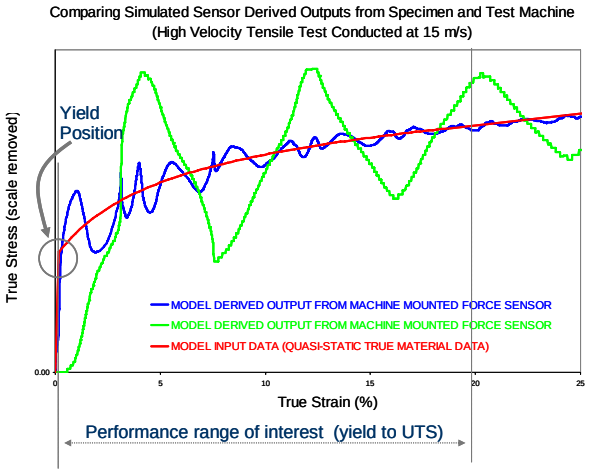

Figure 14: Data Output From Calibrated Model

The yield point defines the transition from elastic to plastic deformation and this must determined with sufficient accuracy for design. The greatest rate of change of stress with strain occurs immediately after yield. But in this low strain region the oscillatory curves have the highest amplitude especially the machine mounted force source sensor, which completely misses the transition zone. On the other hand the specimen mounted force sensor appears to capture the transition zone but yield point is not well defined.

Filtering Technique using Calibrated Model Data for Specimen Mounted forcer Sensor

To create a smooth monotonically increasing flow curve it is necessary to develop a suitable filtering technique. A resulting error may be quantified using the quasi-static reference data. The model output derived from the specimen mounted force sensor (blue hashed curve) is shown in figure 15 with data removed from both ends, leaving a cut zone. The data removed from the right of the curve corresponds to the last peak (or trough) just before maximum stress. Data is also removed to the left of the first peak.

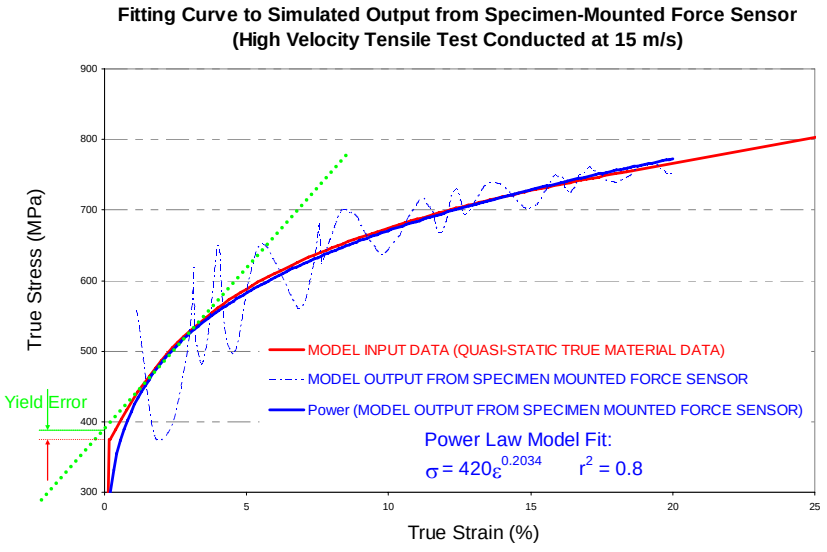

Figure 15:
Curve Fitting

A power law fit through the cut zone of the high frequency model data is identified by the solid blue curve. The quasi-static material input data to model (red curve) is provided as a reference to compare model output data. The trend of the power law curve is consistent with the input data and the error observed is very small at higher strain. The sensitivity of the power law curve fit to precise definition of the length of cut zone in the high frequency data at high strain, leads to a negligible difference (note r^2 value is 0.8). However, an error will be present for the yield point as no clear transition between elastic and plastic deformation is observed with power law model fit. A method to pin point yield could be by taking the first two oscillations which intersect the fitted power law curve highlighted by the green hashed line, and linearly extrapolate to intersect the ordinate axis to locate yield. The error is then determined at less than 3%.

Unfortunately for the machine mounted force sensor, once data is removed to leave a cut zone there is not nearly enough information to fit curve. The r^2 value computed for the fitted curve is $<< 0.1$, which implies that it is highly sensitive to the length of the cut zone at high strain because of the small number of oscillations. Therefore the resulting error is not meaningful because this data is not robust for curve fitting at test speeds conducted at 15 m/s, unlike the specimen mounted force sensor.

Reducing the speed of test for this 25mm gauge length specimen to 5 m/s will increase the number of oscillations from the machine mounted force sensor threefold, when testing the same material and this has been verified by test. However, at 5 m/s the gauge length is usually longer. So typically for a gauge length of 50 mm the total number of oscillations from the machine mounted force sensor would see a six fold increase giving 2.5 (from figure 14) x 6 = 15 oscillations. This is more than the number of oscillations obtained from the specimen mounted force sensor in figure 13, and therefore the machine mounted force sensor output is probably sufficient as far as data interpretation is concerned for tests conducted at 5m/s.

CONCLUDING SUMMARY

A system model of a high speed tensile test conducted at 15 m/s on a servo hydraulic test machine with a fast jaw clamp, to include specimen and sensors in machine and on specimen, has been validated with experimental data.

Validation is based on calibrating the lower frequency response of the machine mounted force sensor, and filtering the higher frequency response of the specimen mounted force sensor as part of post-processing.

The model has enabled a preliminary qualitative ranking of error sources (not included in this paper), in terms of their effects, and recommended current best-practice for high speed testing at 5 and 15 m/s, based on the current IARC specimen designs and fast jaw clamp release position on the moving tab of specimen. It is possible however, that further improvements such as a quantifiable reduction in error may be achieved through either modifying specimen design, or process control enhancements, or both, leading to a more economical testing and characterisation process for materials with measurable strain rate dependency.

Modifying specimen design could include changing the geometry e.g. transition zone radius and/or gauge length to width aspect ratio, to reduce the extent of non-linear elastic stretch at transition zone. Process control enhancements such as reducing the jaw clamp position on moving tab of specimen to reduce wave length (and increase still further the frequency output) to improve accuracy of filtering at low strain. Also the use of velocity profile correction applied to the machine drive signal to reduce variability in the velocity boundary condition, could lead to a measurable reduction in error.

REFERENCES

1. K. Mahadevan, P. Liang, J. Fekete, Effect of Strain Rate in Full Vehicle Frontal Crash Analysis, SAE Technical Paper Series, 2000-01-0625
2. D.M Bruce, D.K.Matlock, J.G.Speer, A.K.De, Assessment of the Strain-Rate Dependent Tensile Properties of Automotive Sheet Steels, SAE Technical Paper Series, 2004-01-0507
3. M. Milititsky, D.K. Matlock, J.G.Speer, C.M.Cady, M.C. Mataya, Effects of Pre-Strain on Properties of Low Carbon Sheet Steels Tested over a Wide Range of Strain Rates, SAE Technical Paper, 2001-01-0082
4. P. Larour, A. Baumer, W. Bleck, High Strain Rate Tensile Testing of Modern Car Body Steels, Steel Future for the Automotive Industry Conference on Steels in cars and Trucks (SCT) c2005.
5. J. Larsson, On modeling of the Strain Rate Effect in Automotive Steels, Steel Future for the Automotive Industry Conference on Steels in cars and Trucks (SCT) c2005.
6. M. Borsutzki, D. Mattissen, T.W. Schaumann, H.J. Sieg, Modern Methods of Material Characterization during the Development of New Steels for Automotive Application, Steel Future for the Automotive Industry Conference on Steels in cars and Trucks (SCT) c2005.
7. D. Cornette, T. Hourman, O. Hudin, J.P.Laurent, A. Reynaert, High Strength Steels for Automotive Safety Parts, SAE Technical Paper Series, 2001-01-0078
8. P.K.C. Wood, C. A. Schley, S. Kenny, T. Dutton. Validating Material Information for Stochastic Crash Simulation Part 1: Quasi-Static Properties, 5th European Ls Dyna Users' Conference. June 2005.
9. BS EN 10002-1:2001 (low speed tensile testing of metallic materials and mechanical property characterisation)
10. VHS 160/100-20 High Strain Rate Test System and Accessories, Instron Ltd, Coronation Rd, High Wycombe, Bucks, England
11. G. E. Dieter, Mechanical Metallurgy, Pub 1988, McGraw-Hill Book Company (UK) Ltd. ISBN 0-07-100406-8
12. International Iron and Steel Institute (IISI) – High Strain Rate Experts Group. Recommendations for Dynamic Tensile Testing of Sheet Steels, pub August 2005.
13. W. Bohme, M. Borsutzki, T. Dupmeier, R. Hacker, P. Larour, U. Mayer, Results of VDEH Round Robin on Guideline SEP 1230 High Velocity Tensile Testing. c2005.
14. K. Hoffmann, An Introduction to Measurements using Strain Gauges, pub 1989, Hottinger Baldwin Messtechnik GmbH, Darmstadt.
15. HBM-UK private correspondence in November 2005
16. Oasys Ls DYNA users manual, Ove Arup and Partners, The Arup Campus, Blythe Valley Park, Solihull, UK
17. Kistler Instruction Manual for Quartz Load Washers, Type 9001-9091A. Kistler Instruments Ltd., Mill Lane, Alton, Hampshire, UK. www. Kistler.com
18. W. T. Thompson, Theory of Vibration with Applications, pub 1981, Pentice-Hall Inc. N.J., ISBN 0-04-620012-6
19. M. Lalanne, P. Berthier, J. D. Hagopian. Mechanical Vibrations for Engineers, pub 1983, John Wiley and Sons Ltd.